

Draw-and-Understand: Leveraging Visual Prompts to Enable MLLMs to Comprehend What You Want

Weifeng Lin^{1*}, Xinyu Wei^{2*}, Ruichuan An³, Peng Gao^{1**}, Bocheng Zou⁴,
Yulin Luo², Siyuan Huang¹, Shanghang Zhang², and Hongsheng Li^{5**}

¹ Shanghai AI Laboratory

² Peking University

³ Xi'an Jiaotong University

⁴ University of Wisconsin-Madison

⁵ The Chinese University of Hong Kong

wflin37@gmail.com,

gaopeng@pjlab.org.cn,

hsli@ee.cuhk.edu.hk

<https://Draw-and-Understand.github.io/>

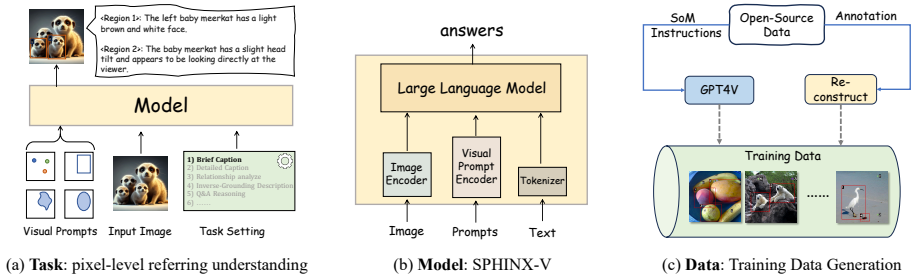


Fig. 1: An Overview of the Draw-and-Understand Project. (a) Illustrating the task of pixel-level referring understanding, where visual prompts and an input image are processed by the model to generate a targeted response. (b) The architecture of SPHINX-V, which consists of an image encoder, a visual prompt encoder, and an LLM. (c) The data generation process for training, which involves two components: reconstruction of open-source data and data generation assisted by GPT-4V.

Abstract. The interaction between humans and artificial intelligence (AI) is a crucial factor that reflects the effectiveness of multimodal large language models (MLLMs). However, current MLLMs primarily focus on image-level comprehension and limit interaction to textual instructions, thereby constraining their flexibility in usage and depth of response. In this paper, we introduce the Draw-and-Understand project: a new model, a multi-domain dataset, and a challenging benchmark for visual prompting. Specifically, we propose SPHINX-V, a new end-to-end trained Multimodal Large Language Model (MLLM) that connects a vision encoder,

* Equal contribution.

** Corresponding authors.

a visual prompt encoder and an LLM for various visual prompts (points, bounding boxes, and free-form shape) and language understanding. To advance visual prompting research for MLLMs, we introduce MDVP-Data and MDVP-Bench. MDVP-Data features a multi-domain dataset containing 1.6M unique image-visual prompt-text instruction-following samples, including natural images, document images, OCR images, mobile screenshots, web screenshots, and multi-panel images. Furthermore, we present MDVP-Bench, a comprehensive and challenging benchmark to assess a model’s capability in understanding visual prompting instructions. Our experiments demonstrate SPHINX-V’s impressive multimodal interaction capabilities through visual prompting, revealing significant improvements in detailed pixel-level description and question-answering abilities.

Keywords: Multimodal Large Language Model · Visual Prompting

1 Introduction

Recent works [2, 33–35, 78] have enhanced Multimodal Large Language Models (MLLMs) with visual perception, facilitating image-related communication and a deeper understanding of the world. However, current MLLMs tend to focus on comprehending entire images by aligning them with textual information at the image level. This method restricts users from highlighting specific areas within images for more detailed inquiries. Therefore, enabling models to understand at the pixel level presents a significant research challenge.

To meet this challenge, recent advancements have concentrated on employing visual prompting to enhance pixel-level comprehension. Specifically, research works [6, 7, 74] utilize textual representations to delineate coordinates within images, thereby enhancing interactions with models. Another group of studies [46, 73, 77] employ positional embeddings to achieve enhanced spatial recognition. Meanwhile, efforts by [4, 51, 67, 70, 73] focus on Regions of Interest (ROI) to augment focus on specific areas within images. Each of these methods has shown promising results, yet they come with their respective limitations. ROI-based methods, for instance, rely on fine-grained masks for precise object representation. However, they often require pre-existing segmentation models or externally provided ground truth masks, which limits user flexibility and model scalability. Furthermore, some methods rely on fixed-format visual prompts such as bounding boxes, which are not user-friendly. A critical shortfall is the inability of most existing methods to support referring to multiple objects simultaneously. This limitation restricts usage flexibility and hampers the achievement of more complex understandings, such as discerning the nuanced interrelations and spatial dynamics among surrounding entities and the backdrop.

To address these shortcomings, we introduce SPHINX-V, an end-to-end multimodal large language model designed to enhance pixel-level image understanding. As depicted in Fig.1(b), the SPHINX-V architecture comprises a vision encoder, a visual prompt encoder, and a Large Language Model (LLM). We

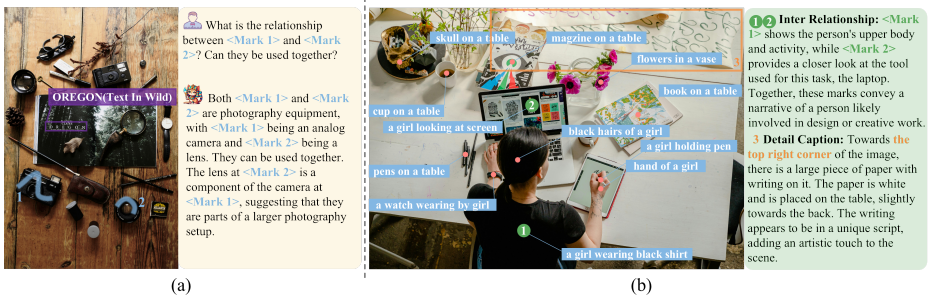


Fig. 2: (a) SPHINX-V has achieved unprecedented performance in text recognition, surpassing other visual prompting MLLMs. Meanwhile, it excels in understanding implicit relationships and conducting complex reasoning. (b) SPHINX-V demonstrates the capability to perceive objects at a pixel level granularity, such as ‘a girl holding a pen’. Furthermore, it can perform detailed captioning and inter-relationship analysis on arbitrarily shaped Regions Of Interest.

leverage pre-trained MLLMs such as SPHINX [18, 32] as the base model, chosen for their robust vision-language understanding. To align vision and language features at the pixel level more effectively, we propose a two-stage training strategy: ($S1$) pre-training for image-visual prompt-text alignment and ($S2$) supervised fine-tuning following instructions. Furthermore, unlike other methods, we integrate continuous visual prompts (like strokes and scribbles) with bounding boxes during inference, avoiding separate modeling. To effectively adapt the model to this approach, we introduce a noise-based training augmentation strategy. This involves adding noise to sparse visual prompts to simulate the region area for free-form shaped inputs. With these methods in place, users can interact with SPHINX-V using their native language, as well as referring actions such as clicking and drawing, to obtain desired answers about the region of interest as shown in Fig. 2.

To further achieve fine-grained pixel-level understanding, high-quality instruction-following training datasets are essential. Currently, several works [67, 70, 74] have developed datasets focused on region-text referring instructions. However, these datasets are mainly limited to natural images, which restricts the model’s applicability after training. Additionally, their scope is often narrow, typically covering only regional descriptions and simple Q&A tasks. To overcome these limitations, we introduce the Multi-domain Visual-Prompting Instruction Dataset (MDVP-Data). Unlike previous datasets, MDVP-Data covers a wider range of image types and interactions, providing a more comprehensive solution. The dataset includes approximately 0.9 million images and 1.6 million query-answer pairs, primarily featuring image-point-text and image-region-text pairings. We assembled this dataset by enhancing existing datasets with segmentation masks or bounding box annotations and by utilizing the capabilities of GPT-4V for data generation. MDVP-Data includes detailed attributes for objects identified by visual prompts, their relationships with nearby entities, and the context within the background. By covering a broad spectrum of pixel-level understanding across

diverse image domains, MDVP-Data significantly improves MLLMs’ adaptability and accuracy in various visual scenarios.

To evaluate the effectiveness and robustness of visual prompting models, we introduce MDVP-Bench, a benchmark tailored for assessing models’ pixel-level comprehension. MDVP-Bench encompasses a variety of tasks, including point-level and region-level captioning, which test the models’ ability to describe specific visual elements; inter-relationship analysis, assessing the understanding of connections between entities; and complex reasoning, challenging the models’ ability to infer and deduce from visual information. We anticipate that MDVP-Bench will lay a solid foundation for future research in the realm of visual prompting and multimodal models.

In particular, our paper makes the following contributions:

- We introduce SPHINX-V, a new multimodal large language model designed for visual prompting, equipped with a novel visual prompt encoder and a two-stage training strategy. SPHINX-V supports multiple visual prompts simultaneously across various types, significantly enhancing user flexibility and achieve a fine-grained and open-world understanding of visual prompts.
- We construct MDVP-Data, a comprehensive dataset for multi-domain visual-prompt instruction tuning. This dataset encompasses data for both point-level and region-level understanding, designed to enhance a model’s comprehension ability and robustness.
- We introduce MDVP-Bench, a challenging benchmark designed to evaluate tasks that require a combination of detailed description referrals, inter-relationship analysis, and complex reasoning.
- In a broad range of pixel-level understanding tasks across established benchmarks, our experimental results reveal that our model consistently outperforms other visual prompting models, showcasing SPHINX-V’s exceptional pixel-level understanding.

2 Related Works

2.1 Multimodal large language models (MLLMs)

In recent years, the development of Large Language Models (LLMs) has marked a significant milestone in the field of Natural Language Processing (NLP). LLMs such as the GPT series [49], PaLM [12], and LLaMA [58] have not only achieved remarkable results in text processing but also laid the foundation for the development of multimodal learning. Following this, the emergence of Multimodal Large Language Models (MLLMs), including BLIP-2 [29], Flamingo [1], and PaLM-E [14], further expanded the application scope of LLMs. Moreover, ongoing research into LLMs has explored extending their capabilities beyond text to other modalities. Notably, a fine-grained understanding of vision has emerged as a new focus. Works such as VisionLLM [62] employ language-guided tokenizers to extract vision features at specific granularities to obtain relevant visual features, showcasing the potential in this direction.

2.2 Visual and Multimodal Prompting

Visual and multimodal prompting in deep learning [3, 24, 67, 70, 74] is an emerging area of study. Techniques using visual prompts (e.g., boxes, masks) aim to enhance model performance on specific visual tasks. Key developments include SAM [24] and its enhanced versions, which support a broad range of prompts. However, SAM initially struggled to generate semantic labels vital for complex scene analysis. This gap led to innovations like SEEM [80], HIPIE [63], and Semantic SAM [27] to improve semantic prediction. However, for real-world applications, models require multidimensional semantic analysis to fully grasp and reason about visual scenes.

Recent studies such as GPT4RoI [73], Kosmos-2 [46], Shikra [7], Ferret [67], and GLaMM [51] have enabled MLLMs to achieve region-based image understanding. Colorful Prompting Tuning (CPT) [66] and RedCircle [55] pioneer the use of color overlays and targeted visual cues to enhance models’ interpretative abilities. ViP-LLaVA [3] also allows users to intuitively mark images and interact with the model using natural prompts. Osprey [70] incorporates fine-grained mask regions into language instruction, achieving precise pixel-wise visual understanding. However, this mask-based technology relies on pre-attached segmentation models or externally provided ground truth masks, which limits its flexibility and scope of application. Furthermore, most existing methods do not support referring to multiple targets simultaneously, which significantly limits the model’s ability to perform more complex understanding and reasoning tasks.

3 MDVP: Multi-domain Visual-Prompt Instruction Data Generation

In this section, we introduce MDVP-Data, an instruction dataset designed to foster fine-grained pixel-level and open-world image understanding in MLLMs, encompassing approximately 1.6 million multimodal dialogues. MDVP-Data integrates both point-level and region-level instruction data derived from public datasets. It consists of two types of data: (1) a restructured public grounding dataset formatted for visual prompt-based instruction following (Sec. 3.1); and (2) high-quality training pairs developed using meticulously crafted prompt templates, produced through the GPT-4V model (Sec. 3.2). Additionally, we present MDVP-Bench, a challenging benchmark suite designed to evaluate comprehensive pixel-level understanding capabilities under various visual prompts.(Sec. 3.3)

3.1 Inverse-Grounding Visual Prompt-based Dataset

We observe that the grounding capability, which encompasses the ability to localize visual content and link each entity referred to by a noun phrase in the caption to a specific region in the image, essentially represents the inverse process of visual prompt proficiency. Building on this insight, we reorganize existing datasets for Referring Expression Comprehension (REC), Phrase Grounding, and Grounding QA to construct our dataset for visual prompting.

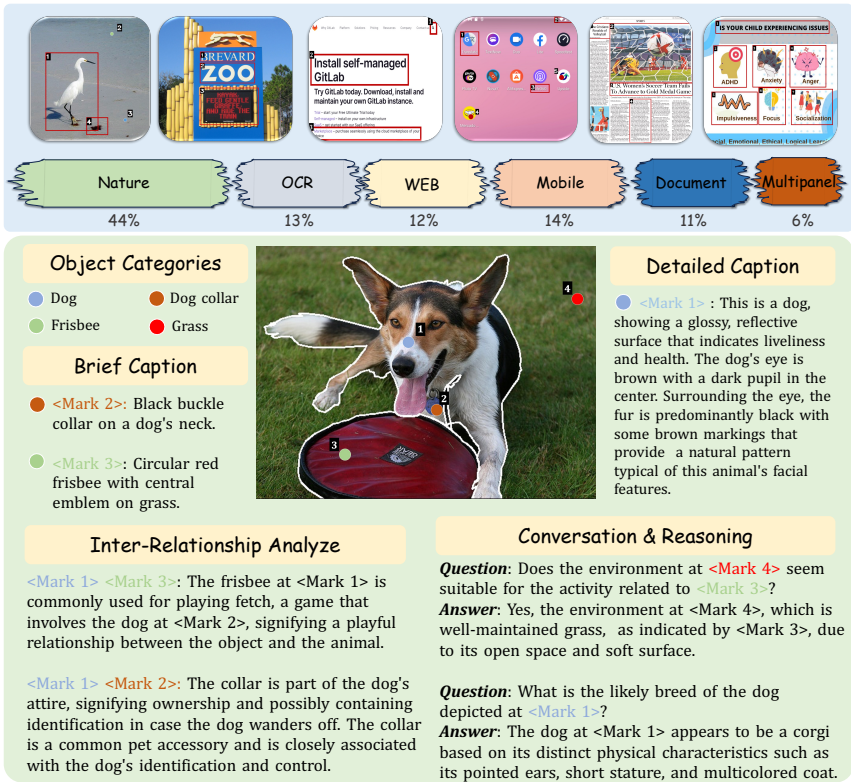


Fig. 3: Illustrative Example from the MDVP Dataset: This diagram displays the distribution of images drawn from various domains, including nature scenes, texts in the wild, web content, mobile interfaces, documents, and multi-pane graphics. It also features a sample from the GPT-assisted MDVP dataset, emphasizing the diversity and richness of its point-based and region-based instruction-following data.

For captioning tasks, we have inverted the inputs and outputs of existing REC and Phrase Grounding datasets, such as Flickr30K [48] RefCOCO/+ [23, 69] GCG [51], and GRIT [46], treating the ground truth boxes as input visual prompts, with the corresponding natural language descriptions serving as the answers. For visual prompt-based conversations, we utilize grounding QA pairs from point-QA [40], Visual 7W [79] and VCR [72] datasets. The bounding boxes mentioned in the questions are treated as visual prompt inputs, with the positions of bounding boxes in both questions and answers being substituted with **<Mark *i*>** or **<Region *i*>**.

3.2 GPT4V-assisted Visual Instruction Data Generation

To construct a more comprehensive and diverse instruction-following dataset, we have collected various multi-domain images along with their unique annota-

tions from publicly available datasets. These encompass natural images, Optical Character Recognition (OCR) in the wild, documents, webpage screenshots, mobile screen captures, and multi-panel images. For each distinct image domain, we have meticulously crafted prompts to facilitate the GPT-4V’s adoption of various roles in the generation of instructional data. Specifically, we task GPT-4V with four distinct assignments: brief captioning, detailed captioning, inter-relationship analysis, and the generation of complex reasoning. Uniquely, the captions created for each image type possess their own distinctive characteristics. For instance, in mobile screen captures, objects can be identified not only as relevant components—icons, text, search bars, URLs, etc.—but information about potential actions is also provided. This includes whether a component is clickable and the expected outcome upon interaction. This diversity significantly enhances the richness and presents challenges for our dataset, covering a broader and more comprehensive range of knowledge domains.

Furthermore, as shown in Fig. 3, to enable GPT-4V to better recognize the objects referred to by visual prompts, we have employed Set-of-Marks (SoM) [65] prompting. This method involves directly marking the highlighted objects on the input images, ensuring that the data created is strongly associated with the referenced objects. Concurrently, we propose incorporating the category information of each object within the prompts, which significantly enhances the quality of the generated data. (For more details on the specific prompts and the methods used for marking the objects, please refer to the Appendix. C.2.)

3.3 MDVP-Bench

To evaluate the proficiency of the MLLM in complex pixel-level image understanding tasks and its versatility across various domains, we initially curated a subset of our MDVP-Data. This subset was subjected to a thorough manual content review and filtering process, culminating in the creation of MDVP-Bench. MDVP-Bench is a comprehensive and challenging benchmark encompassing a wide array of tasks, including concise descriptions, elaborate narratives, analyses of interconnections among different regions, and complex reasoning.

Existing evaluations typically follow the approach of LLaVA [35], utilizing GPT-4 for open-ended evaluation and employing textual descriptions to depict image content. These textual descriptions, often based on image annotations, can lead to scenarios where GPT-4 may not recognize objects or backgrounds not annotated in the scene. Additionally, inherent domain gaps between textual descriptions and images can lead to GPT-4 misunderstanding the image content. To address these limitations, we employ GPT-4V for evaluation in MDVP-Bench. Following the pipeline described in Sec.3.2, we directly annotate images with SoM prompting, submitting both the image and textual questions to GPT-4V for scoring. This approach helps to circumvent potential misinterpretations of image content by GPT-4V. The scoring adheres to the LLaVA-bench guidelines, with scores ranging from 1 to 10, where higher scores indicate superior model performance.

4 Model Architecture

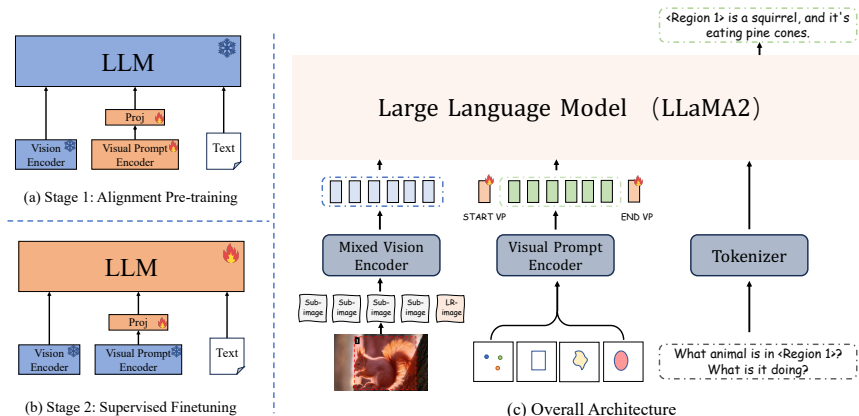


Fig. 4: Overview of the SPHINX-V model architecture. (a & b) The proposed two-stage training strategy. **(c)** Overall model architecture.

In this section, we present SPHINX-V, a model designed for pixel-level referring understanding. As illustrated in Fig. 4(c), SPHINX-V comprises three components: a mixed vision encoder, a versatile visual prompt encoder, and a large language model (LLM). Given an image alongside coordinates of specific points or regions and instruction language, we perform tokenization and encoding to derive three distinct embeddings: image embeddings Z_i , visual prompt embeddings Z_v , and text embeddings Z_t . Subsequently, we employ two projection matrices to convert Z_i and Z_v into language embedding tokens, aligning them with the word embedding space in the language model. Finally, we integrate the image, visual prompt, and language representations, forwarding them collectively to the LLM to attain pixel/region-level understanding capability.

Vision Encoder. Driven by the scalability and effective pretraining of MLLMs, we incorporate the Mixed Vision Encoder (MVE) from the pretrained SPHINX [18, 32]. This encoder generates the image embeddings $Z_i = MVE(X_i)$, operating at an image resolution of 448×448 . It expands the scope of image embeddings to encompass multiple scales and high-resolution sub-images, facilitating the efficient encoding of high-resolution images.

Visual Prompt Encoder. In SPHINX-V, we mainly consider two types of visual prompts: points and bounding boxes. As shown in Fig. 4(c), we introduce a new visual prompt encoder. Inspired by SAM [24], initially, we utilize positional encodings [57] for points and boxes, then adds learnable embeddings for each prompt type, and finally processes them through a linear layer to obtain unified output embeddings. Additionally, our visual prompt encoder accommodates a dynamic number of visual prompts as input. Specifically, we first set a fixed number of input tokens for visual prompts (e.g., 10). Then, based on the validity of the actual input tokens, we equip both valid and invalid tokens with a set of learnable vectors to assist the model in discerning their effective features. (For more details on the visual prompt encoder, please refer to the Appendix. A.)

Large Language Model. We consider LLaMA 2-13B [58] as our large language model (LLM), a transformer-based decoder-only LLM.

Table 1: Statistics of Data in Stage 1.

Type	Raw Data	#Samples
Natural	COCO [31]/LVIS [19]	4.6M
	Visual Genome [25]	
	OpenImages [26]	
	Obj365 [54]/V3Det [60]	
	ADE20k [76]	
	Cityscapes [13]	
	Pascal VOC [41]	
Flickr30k [48]		
Document layout	Docbank [30]	3.1M
	PublayNet [75]	
	DoclayNet [47]/M6Doc [9]	
OCR Spotting	icdar13 [22]/icdar15 [21]	550K
	ctw1500 [71]/mlt2017 [43]	
	mlt2019 [42]/totaltext [11]	
	CurvedSynText150k [36]	
Android & Web	AITW [52]/SeeClick [10]	300K

Table 2: Statistics of Data in Stage 2.

Task	Raw Data	#Samples
Category Identification	Subset in Stage-1	2.0M
Brief Caption	RefCOCO [23, 69]	1.2M
	RefCOCO+ [23, 69]	
	RefCOCOg [23, 69]	
Detailed Caption	Visual Genome [25]	752K
	MDVP-Data	
Relationship Analysis	MDVP-Data	1.1M
	Visual Genome [25]	
Inverse-Grounding Description	GRIT [46]	1.2M
	Flicker30K [48]	
	OpenPsgGCG [51]	
Whole Image Caption	shareGPT4v [8]	1.2M
	laionGPT4v [5]	
Q&A and Resoning	VCR [25]/Visual7W [79]	2.3M
	Osprey-724K [70]	
	MDVP-Data	

Training Strategy. The training process of our SPHINX-V model consists of two important stages.

- **Stage 1: Image-Visual Prompt-Text Alignment Pre-training.** By employing a visual prompt encoder, we initially freeze both the pre-trained vision encoder and the pre-trained LLM. Then, we focus on training the features of visual prompts to align with the features of image-visual prompt-text. Following the approach in LLaVA [35], we implement an MLP as the connector between visual prompts and language to enhance the multimodal prompting capabilities of the model. At the first stage, we gather and reconstruct open-source datasets, including those for object detection, semantic segmentation, layout detection, spotting, and more, to build our training data. Specifically, for point inputs, we initially randomly sample from semantic segmentation images, where each point has a corresponding pixel-level label annotation. Similarly, for instance segmentation, we can sample points from the mask of each object, with these points corresponding to the label annotation of that object. For box inputs, we directly utilize the ground truth bounding boxes provided by detection datasets as visual prompt inputs, allowing the model to recognize their corresponding labels. The structure of our stage-1 pre-training data is as follows:

```

{"from": "human", "value": "Please identify the labels of each marked point in the image. "},
{"from": "GPT", "value": "<Mark 1>: Label 1\n< Mark 2>: Label 2\n< Mark 3>: Label 3\n....."}

{"from": "human", "value": "Please identify the labels of each marked region in the image. "},
{"from": "GPT", "value": "<Region 1>: Label 1\n< Region 2>: Label 2\n< Region 3>: Label 3\n....."}

```

As illustrated in Table 1, we have gathered a diverse array of detection and segmentation datasets covering multiple image domains. These datasets encompass a wide range of label types, including elements of the natural world (persons, animals, stuff, etc.), document elements (titles, paragraphs, images, tables, etc.), OCR (text recognition), and screenshots (icons, text, search bars, etc.). With

such rich and extensive data for pre-training, SPHINX-V is equipped to develop capabilities for visual prompting and preliminary category identification.

Furthermore, to support free-form shape visual prompts, we propose a noise-based training augmentation in the pre-training stage to simulate the region area required when inputting free-form shaped visual prompts. Specifically, for box-type visual prompts, we introduce a certain degree of noise based on the size of the box itself. This noise may cause the ground truth bounding box to be slightly larger than the target object or only cover part of the target object, thereby approximating a free-form outer rectangle. For points, we sample several pixels within the mask of a target object. These pixels are directed towards the same target object during training, thus achieving precise point-based referring.

• **Stage 2: Multi-Task Supervised Finetuning.** At the second stage, we load the weights trained during stage 1 and keep the vision encoder and visual prompt encoder weights frozen. We then fine-tune the visual prompt projector and the LLM model. Our focus is on enhancing SPHINX-V’s ability to accurately interpret user instructions and handle diverse pixel-level understanding tasks, such as detailed captioning, inter-relationship analysis, and complex reasoning. Table 2 outlines all the data utilized during stage 2 fine-tuning, which includes our proposed MDVP dataset, Visual Genome (VG) [25], Visual Commonsense Reasoning (VCR) [72], Visual7w [79], and Osprey-724k [70]. Furthermore, we reformat the grounding dataset for compatibility with visual prompt-based instructions. Lastly, we ensure the model retains the capability to provide detailed captions for the entire image when given a visual prompt that encompasses most of the image’s content. After the instruction fine-tuning in stage 2, SPHINX-V becomes proficient in comprehending complex scenarios based on user instructions and specific regions of interest.

Inference. Although SPHINX-V is limited to modeling point-level and box-level features of visual prompts, the noise-based training augmentation proposed in the stage 1 enables users to freely draw on the image, greatly increasing the flexibility of user usage. Specifically, by pre-processing these free-form visual prompts, we can obtain their corresponding bounding boxes, and then feed these box coordinates into SPHINX-V for inference.

5 Experiments

5.1 Implementation Details

We utilized AdamW [38] as our optimizer and employed flash attention [16] to improve computational efficiency. During the first stage of training, we set the initial learning rate to $4e - 5$. For the second stage, the learning rate was adjusted to $1e - 5$. The input images were processed at a resolution of 448 x 448 pixels, and the maximum sequence length for the Large Language Model (LLM) was established at 2048. The entire training procedure was conducted on 8 NVIDIA A100 GPUs, each equipped with 80GB of memory. For all evaluation experiments, we opted for a zero-shot testing approach, refraining from further fine-tuning on specific datasets.

Table 3: The results of referring object classification on LVIS and PACO.

Method	LVIS		PACO	
	Semantic Similarity	Semantic IoU	Semantic Similarity	Semantic IoU
LLaVA-1.5 [34]	48.95	19.81	42.20	14.56
Kosmos-2 [46]	38.95	8.67	32.09	4.79
Shikra-7B [7]	49.65	19.82	43.64	11.42
GPT4RoI-7B [73]	51.32	11.99	48.04	12.08
Ferret-7B [67]	63.78	36.57	58.68	25.96
Osprey-7B [70]	65.24	38.19	73.06	52.72
SPHINX-V(Point)	83.16	58.64	76.18	51.13
SPHINX-V(Box)	87.06	62.90	79.88	55.04

5.2 Referring Object Classification

This task is defined as follows: the question targets a specific area within the image, requiring the model to identify the object within that designated region. Following [70], we employ two semantic relevance indicators—Semantic Similarity (SS) and Semantic Intersection over Union (S-IoU) [53]—to assess a model’s classification prowess on the validation sets of object-level LVIS [19] and part-level PACO [50] datasets. As the results shown in Table 3 indicate, SPHINX-V achieves 83.16% in SS and 58.64% in S-IoU based on point-level visual prompts, and 87.06% in SS and 62.90% in S-IoU based on box-level visual prompts on the LVIS dataset. Both sets of results significantly outperform the state-of-the-art method by a notable margin. Furthermore, SPHINX-V surpasses the previous best, Osprey, by 6.82% in SS and 2.32% in S-IoU on the PACO dataset, demonstrating its robust capability in fine-grained part-level classification.

We also conducted tests on traditional closed-set object classification tasks. To ensure the model outputs names of categories within the closed set, we followed the approach described in Ferret [67] and adapted our evaluation to a binary-choice format. We posed questions such as *‘Please identify the label of the marked region in the image. Is it (Class A) or (Class B)?’*. The results, as shown in Table 4, further demonstrate SPHINX-V’s excellent classification ability.

5.3 Regional Optical Character Recognition.

Optical character recognition (OCR) is a task focused on identifying text in images, serving as a fundamental aspect of visual entity recognition. Following [74], we utilize the COCO-Text dataset [59] to gauge the regional text recognition prowess of SPHINX-V. Employing the ground-truth bounding boxes supplied within the dataset, we prompt the model with requests such as *‘Please provide the ocr results of each marked region in the image.’* SPHINX-V then analyzes and response the textual content present within the specified regions. Given that most visual prompt-based models do not support OCR, we compare our results with ChatSpot under identical zero-shot settings. As illustrated in Table 4, our

Table 4: Results of referring object classification and optical character recognition (OCR) on COCO text. We randomly perturb the center positions and scale the dimensions of box visual prompts to simulate free-form prompts.

Method	LVIS			OCR (COCO Text)
	Point	Box	Free-Form	Box
LLaVA [34]	50.1	50.3	-	-
Kosmos-2 [46]	-	60.3	-	-
Shikra-7B [7]	57.8	67.7	-	-
GPT4RoI-7B [73]	-	61.8	-	-
Ferret-7B [67]	67.9	79.4	69.8	-
Ferret-13B [70]	68.4	80.5	71.0	-
ChatSpot-7B	-	64.5	-	31.8
SPHINX-V(Ours)	86.46	89.82	88.96	45.44

Table 5: Detailed region-level captioning performance on the RefCOCOg validation set.

Method	Detailed Description
LLaVA-1.5 [34]	71.11
Kosmos-2 [46]	40.89
Shikra-7B [7]	40.97
GPT4RoI-7B [73]	49.97
Osprey-7B [70]	77.54
SPHINX-V(Ours)	92.19

Table 6: Brief region captioning performance evaluated on the validation set of RefCOCOg.

Method	Type	METEOR	CIDEr
GRIT [67]	Box	15.2	71.6
Kosmos-2 [46]	Box	14.1	62.3
GLaMM [51]	Box	16.2	105.0
Osprey-7B [70]	Mask	16.6	108.3
SPHINX-V(Ours)	Box	23.9	162.5

model surpasses the ChatSpot by 13.64%, showcasing the promising regional capability of text recognition.

Moreover, as shown in the Fig. 5, SPHINX-V is capable of not only recognizing text in the referring region but also possesses enhanced understanding and descriptive abilities. For instance, it can further describe characteristics such as the font type, color, and background of the text, and understand the role of the text within the image area. This fully demonstrates SPHINX-V’s exceptional pixel-level understanding capabilities.

5.4 Region-Level Captioning

Brief Region Description. We provide quantitative comparisons for the region-level captioning task using both mask- and box-based approaches [15, 46, 51, 70]. Specifically, we employ a box visual prompt and a text prompt, such as *"Please provide a brief description of each marked region in the image,"* to prompt SPHINX-V to concisely describe the content of the targeted region. Experiments were conducted on the validation sets of RefCOCOg. The comparison results, shown in Table 6, demonstrate promising outcomes when compared to other methods. (More experimental results can be found in Appendix. B.1)

Table 7: Results on LLaVA-Bench and Ferret-Bench.

	LLaVA-Bench			Ferret-Bench	
	Conversation	Detail Description	Complex Reasoning	Referring Description	Referring Reasoning
LLaVA [35]	85.4	68.3	92.1	41.4	31.7
Kosmos-2 [46]	71.7	63.4	74.9	51.8	33.7
Shikra-7B [7]	80.6	70.7	88.1	46.0	41.6
Ferret-7B [67]	84.4	79.4	96.3	68.7	67.3
Ferret-13B [67]	85.2	80.9	96.4	70.6	68.7
SPHINX-V(Ours)	85.0	86.4	91.3	76.4	70.4

Table 8: Results on different domains of MDVP-bench. *Osprey accepts the ground truth mask of the referring object as visual prompt input.

Domain	Natural		OCR		Multi-panel		Screenshot	
	Box	Point	Box	Point	Box	Point	Box	Point
Osprey* [70]	86.40	-	18.33	-	48.56	-	28.84	-
Ferret-7B [67]	84.92	81.42	21.24	12.20	44.42	32.08	26.40	10.62
Ferret-13B [67]	86.67	83.40	27.68	12.20	49.83	37.65	30.92	14.40
SPHINX-V(Ours)	88.82	92.95	78.49	76.29	77.30	79.08	80.07	54.05

Detailed Region Description. To further evaluate the detailed area description capabilities of our model and other visual prompting MLLMs, inspired by [34, 70], we leverage GPT-4 to comprehensively measure the quality of the responses generated by the model to the input referring regions. Specifically, in the same manner as Osprey [70], we sample 80 images from the validation set of RefCOCOs [23, 69] for generating detailed region caption, using box visual prompt and text prompt like *"Please provide a detailed description of each marked region in the image."* Subsequently, GPT-4 was utilized to assess the detailed captions generated by MLLMs. The evaluation scores span from 1 to 10, with higher scores reflecting enhanced performance. To evaluate the efficacy of MLLMs, we determined the ratio of the predicted answer score to that of GPT-4, expressing this ratio as a percentage. The results shown in Table 5 indicates that SPHINX-V achieves the best performance with 92.19% accuracy, significantly outperforming other region-based and mask-based methods.

5.5 Comprehensive Assessment: LLaVA-Bench, Ferret-Bench and MDVP-Bench

We use LLaVA-Bench to compare SPHINX-V with previous models [7, 34, 46, 70] to evaluate whole image-level understanding capability. Given that the questions in LLaVA-Bench are based on the whole image, we employ bounding boxes of nearly full-image size as visual prompts. Furthermore, we use Ferret-Bench and our proposed MDVP-Bench to evaluate pixel-level understanding capability. Experiments were conducted on the Referring Description and Referring Reasoning tasks within Ferret-Bench.

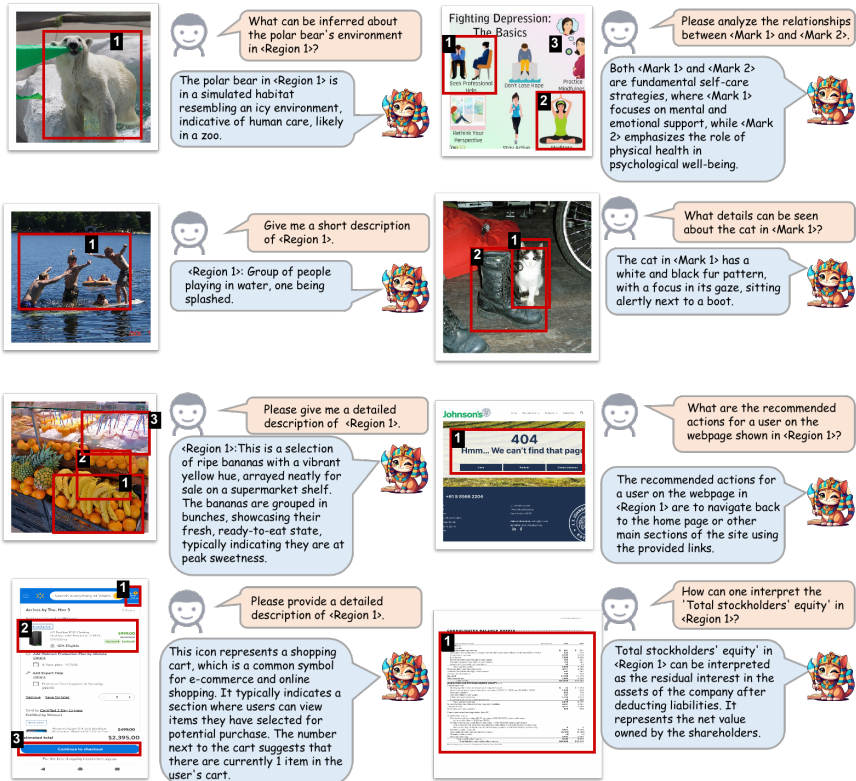


Fig. 5: Visual examples of SPHINX-V.

As the results presented in Table 7, since we did not incorporate open-source image-level VQA data into our training dataset, it is observable that in LLaVA-Bench, our model performs slightly below the current state-of-the-art methods in conversation and complex reasoning evaluations. However, it still significantly leads in the capability of detailed captioning. Moreover, in the Ferret-Bench assessment focused on pixel-level image understanding, whether in referring description or referring reasoning, our model achieved the best performance. This demonstrates SPHINX-V's powerful fine-grained part-level understanding and reasoning abilities.

For MDVP-Bench, we mixed different tasks together to obtain a comprehensive assessment of the model's overall capabilities, applying evaluation process mentioned in Sec 3.3. As the results shown in Table 8, compared to Osprey and Ferret, our SPHINX-V significantly leads in evaluations across multiple domains. In addition, it can be observed that the scores for box prompts are sometimes lower than those for point prompts. Upon reviewing the responses to each question, we discovered that for tasks with fewer visual prompts on an image, box-based prompts perform better, while in tasks involving more visual prompts on an image, simple point prompts demonstrate significantly better performance. This finding reveals the modeling function of our visual prompt encoder and

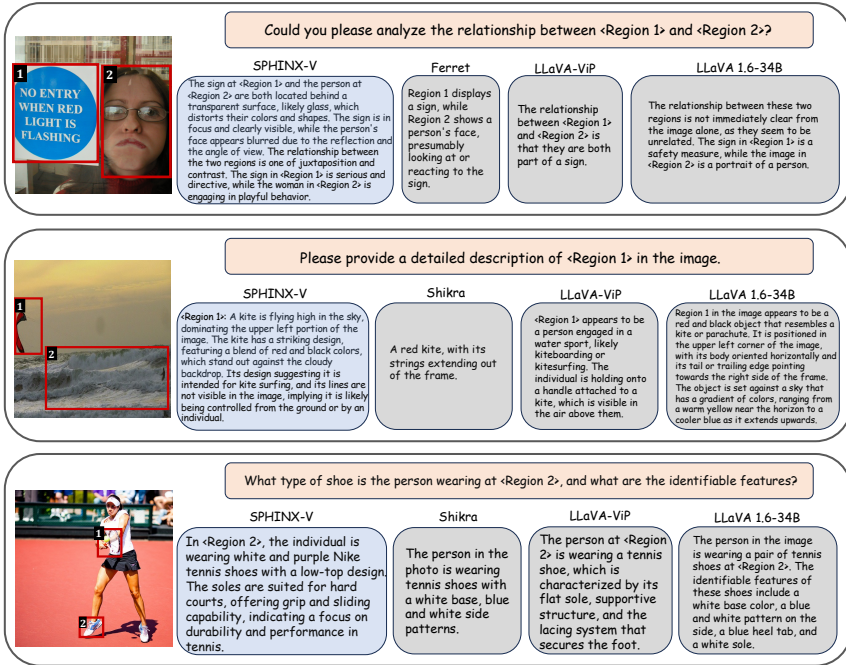


Fig. 6: Comparative visual examples from various methods.

their capability to model different visual prompts, inspiring future research and improvement of their functionality.

5.6 Visualization

We provide visual examples to further illustrate the pixel-level spatial understanding capabilities of our SPHINX-V across a diverse range of visual prompts. Fig. 5 displays a variety of visual scenarios from different domains, such as natural scenes, mobile and web interfaces, optical character recognition (OCR) in natural settings, document layouts, and multi-panel images. In these complex situations, SPHINX-V showcases its proficiency in accurately responding to queries, highlighting its robust and versatile capabilities. (More visualizations could be found in Appendix. 9)

Furthermore, Fig. 6 provides comparisons with existing image-level and region-level methods. Our methodology yields superior scene comprehension results, offering a nuanced and detailed analysis when compared to existing image-level and region-level approaches.

5.7 Ablation Study

To evaluate the effectiveness of the key elements of our design, we conduct the following ablation experiments. Given the extensive amount of training data, our comparison was limited to the first 50k training iterations.

Table 9: Comparisons across different modeling format of visual prompts and training strategy.

Method	LVIS		PACO	
	Semantic Similarity	Semantic IoU	Semantic Similarity	Semantic IoU
Alpha Blending	45.5	21.7	39.6	14.2
Text	47.3	25.5	43.47	18.3
Encoder(Ours)	55.9	30.1	52.3	22.4
One-Stage	43.1	19.2	39.2	12.5
Two-Stage(Ours)	55.9	30.1	52.3	22.4

The Effectiveness of Visual Prompt Encoder. To assess the effectiveness of our visual prompt encoder, we explored two alternative methods for incorporating visual prompts into MLLMs: (1) overlaying the visual prompts on the original image via alpha blending with an alpha value of 0.5; and (2) explicitly including the coordinates of the visual prompt in the instructional text prompt. As shown in Table 9, while these alternative methods enabled the MLLM to successfully identify the regions indicated by the visual prompts, their performance was not as strong as that achieved with our visual prompt encoder. This suggests that our visual prompt encoder possesses superior capabilities for processing visual prompts.

The two-stage Training Strategy. To validate the effectiveness of our proposed two-stage training strategy, we conducted experiments in which we bypassed the pre-training phase (stage 1) and directly set both the visual prompt encoder and the LLM to a trainable state for model training. As depicted in Table 9, the results clearly demonstrate that, within the same training duration and using identical data, the two-stage training approach significantly outperforms the single-stage method. This improvement is due to the two-stage training strategy’s notable acceleration of the model’s convergence speed, thereby underscoring the effectiveness and necessity of the two-stage training paradigm.

6 Conclusion

In summary, we introduce a new multimodal large language model for visual prompting named SPHINX-V, which exhibits promising capabilities in pixel-level image understanding. With our proposed visual prompt encoder and two-stage training strategy, SPHINX-V is able to support various types of visual prompts, including points, boxes, and free-form shapes, significantly enhancing user flexibility. Additionally, we have curated the MDVP dataset, comprising 1.6M high-quality image-point-text and image-region-text pairs for model training, and the MDVP benchmark, which is both comprehensive and challenging, for evaluation purposes. Our superior performance in established visual prompting tasks—including referring object classification, region-level captioning, regional OCR, and referring reasoning—underscores the efficacy and robustness of SPHINX-V. We anticipate that our contributions will lay a solid foundation for further exploration in the field of intelligent visual interaction systems.

References

1. Alayrac, J.B., Donahue, J., Luc, P., Miech, A., Barr, I., Hasson, Y., Lenc, K., Mensch, A., Millican, K., Reynolds, M., et al.: Flamingo: a visual language model for few-shot learning. *Advances in Neural Information Processing Systems* **35**, 23716–23736 (2022) [4](#)
2. Bai, J., Bai, S., Yang, S., Wang, S., Tan, S., Wang, P., Lin, J., Zhou, C., Zhou, J.: Qwen-vl: A frontier large vision-language model with versatile abilities. *arXiv preprint arXiv:2308.12966* (2023) [2](#)
3. Cai, M., Liu, H., Mustikovela, S.K., Meyer, G.P., Chai, Y., Park, D., Lee, Y.J.: Making large multimodal models understand arbitrary visual prompts. *arXiv preprint arXiv:2312.00784* (2023) [5](#), [24](#)
4. Chen, C., Qin, R., Luo, F., Mi, X., Li, P., Sun, M., Liu, Y.: Position-enhanced visual instruction tuning for multimodal large language models. *arXiv preprint arXiv:2308.13437* (2023) [2](#)
5. Chen, G.H., Chen, S., Zhang, R., Chen, J., Wu, X., Zhang, Z., Chen, Z., Li, J., Wan, X., Wang, B.: Allava: Harnessing gpt4v-synthesized data for a lite vision-language model. *arXiv preprint arXiv:2402.11684* (2024) [9](#)
6. Chen, J., Zhu, D., Shen, X., Li, X., Liu, Z., Zhang, P., Krishnamoorthi, R., Chandra, V., Xiong, Y., Elhoseiny, M.: Minigtpt-v2: large language model as a unified interface for vision-language multi-task learning. *arXiv preprint arXiv:2310.09478* (2023) [2](#)
7. Chen, K., Zhang, Z., Zeng, W., Zhang, R., Zhu, F., Zhao, R.: Shikra: Unleashing multimodal llm’s referential dialogue magic. *arXiv preprint arXiv:2306.15195* (2023) [2](#), [5](#), [11](#), [12](#), [13](#)
8. Chen, L., Li, J., Dong, X., Zhang, P., He, C., Wang, J., Zhao, F., Lin, D.: Sharegpt4v: Improving large multi-modal models with better captions. *arXiv preprint arXiv:2311.12793* (2023) [9](#)
9. Cheng, H., Zhang, P., Wu, S., Zhang, J., Zhu, Q., Xie, Z., Li, J., Ding, K., Jin, L.: M6doc: A large-scale multi-format, multi-type, multi-layout, multi-language, multi-annotation category dataset for modern document layout analysis. In: *Proceedings of the IEEE/CVF Conference on Computer Vision and Pattern Recognition*. pp. 15138–15147 (2023) [9](#)
10. Cheng, K., Sun, Q., Chu, Y., Xu, F., Li, Y., Zhang, J., Wu, Z.: Seeclck: Harnessing gui grounding for advanced visual gui agents. *arXiv preprint arXiv:2401.10935* (2024) [9](#)
11. Ch’ng, C.K., Chan, C.S.: Total-text: A comprehensive dataset for scene text detection and recognition. In: *2017 14th IAPR international conference on document analysis and recognition (ICDAR)*. vol. 1, pp. 935–942. IEEE (2017) [9](#)
12. Chowdhery, A., Narang, S., Devlin, J., Bosma, M., Mishra, G., Roberts, A., Barham, P., Chung, H.W., Sutton, C., Gehrmann, S., et al.: Palm: Scaling language modeling with pathways. *Journal of Machine Learning Research* **24**(240), 1–113 (2023) [4](#)
13. Cordts, M., Omran, M., Ramos, S., Rehfeld, T., Enzweiler, M., Benenson, R., Franke, U., Roth, S., Schiele, B.: The cityscapes dataset for semantic urban scene understanding. In: *Proceedings of the IEEE conference on computer vision and pattern recognition*. pp. 3213–3223 (2016) [9](#)
14. Driess, D., Xia, F., Sajjadi, M.S., Lynch, C., Chowdhery, A., Ichter, B., Wahid, A., Tompson, J., Vuong, Q., Yu, T., et al.: Palm-e: An embodied multimodal language model. *arXiv preprint arXiv:2303.03378* (2023) [4](#)

15. Duckworth, A.L., Quinn, P.D.: Development and validation of the short grit scale (grit-s). *Journal of personality assessment* **91**(2), 166–174 (2009) [12](#)
16. Ford, S., Cova, M., Kruegel, C., Vigna, G.: Analyzing and detecting malicious flash advertisements. In: 2009 Annual Computer Security Applications Conference. pp. 363–372. IEEE (2009) [10](#)
17. Gan, Z., Chen, Y.C., Li, L., Zhu, C., Cheng, Y., Liu, J.: Large-scale adversarial training for vision-and-language representation learning. *Advances in Neural Information Processing Systems* **33**, 6616–6628 (2020) [24](#)
18. Gao, P., Zhang, R., Liu, C., Qiu, L., Huang, S., Lin, W., Zhao, S., Geng, S., Lin, Z., Jin, P., et al.: Sphinx-x: Scaling data and parameters for a family of multi-modal large language models. *arXiv preprint arXiv:2402.05935* (2024) [3](#), [8](#), [23](#)
19. Gupta, A., Dollar, P., Girshick, R.: Lvis: A dataset for large vocabulary instance segmentation. In: Proceedings of the IEEE/CVF conference on computer vision and pattern recognition. pp. 5356–5364 (2019) [9](#), [11](#)
20. Huang, X., Wang, J., Tang, Y., Zhang, Z., Hu, H., Lu, J., Wang, L., Liu, Z.: Segment and caption anything. *arXiv preprint arXiv:2312.00869* (2023) [24](#)
21. Karatzas, D., Gomez-Bigorda, L., Nicolaou, A., Ghosh, S., Bagdanov, A., Iwamura, M., Matas, J., Neumann, L., Chandrasekhar, V.R., Lu, S., et al.: Icdar 2015 competition on robust reading. In: 2015 13th international conference on document analysis and recognition (ICDAR). pp. 1156–1160. IEEE (2015) [9](#)
22. Karatzas, D., Shafait, F., Uchida, S., Iwamura, M., i Bigorda, L.G., Mestre, S.R., Mas, J., Mota, D.F., Almazan, J.A., De Las Heras, L.P.: Icdar 2013 robust reading competition. In: 2013 12th international conference on document analysis and recognition. pp. 1484–1493. IEEE (2013) [9](#)
23. Kazemzadeh, S., Ordonez, V., Matten, M., Berg, T.: Referitgame: Referring to objects in photographs of natural scenes. In: Proceedings of the 2014 conference on empirical methods in natural language processing (EMNLP). pp. 787–798 (2014) [6](#), [9](#), [13](#)
24. Kirillov, A., Mintun, E., Ravi, N., Mao, H., Rolland, C., Gustafson, L., Xiao, T., Whitehead, S., Berg, A.C., Lo, W.Y., et al.: Segment anything. *arXiv preprint arXiv:2304.02643* (2023) [5](#), [8](#), [23](#)
25. Krishna, R., Zhu, Y., Groth, O., Johnson, J., Hata, K., Kravitz, J., Chen, S., Kalantidis, Y., Li, L.J., Shamma, D.A., et al.: Visual genome: Connecting language and vision using crowdsourced dense image annotations. *International journal of computer vision* **123**, 32–73 (2017) [9](#), [10](#), [24](#)
26. Kuznetsova, A., Rom, H., Alldrin, N., Uijlings, J., Krasin, I., Pont-Tuset, J., Kamali, S., Popov, S., Mallocci, M., Kolesnikov, A., et al.: The open images dataset v4: Unified image classification, object detection, and visual relationship detection at scale. *International Journal of Computer Vision* **128**(7), 1956–1981 (2020) [9](#)
27. Li, F., Zhang, H., Sun, P., Zou, X., Liu, S., Yang, J., Li, C., Zhang, L., Gao, J.: Semantic-sam: Segment and recognize anything at any granularity. *arXiv preprint arXiv:2307.04767* (2023) [5](#)
28. Li, G., Duan, N., Fang, Y., Gong, M., Jiang, D.: Unicoder-vl: A universal encoder for vision and language by cross-modal pre-training. In: Proceedings of the AAAI conference on artificial intelligence. vol. 34, pp. 11336–11344 (2020) [24](#)
29. Li, J., Li, D., Savarese, S., Hoi, S.: Blip-2: Bootstrapping language-image pre-training with frozen image encoders and large language models. *arXiv preprint arXiv:2301.12597* (2023) [4](#)
30. Li, M., Xu, Y., Cui, L., Huang, S., Wei, F., Li, Z., Zhou, M.: Docbank: A benchmark dataset for document layout analysis. *arXiv preprint arXiv:2006.01038* (2020) [9](#)

31. Lin, T.Y., Maire, M., Belongie, S., Hays, J., Perona, P., Ramanan, D., Dollár, P., Zitnick, C.L.: Microsoft coco: Common objects in context. In: Computer Vision–ECCV 2014: 13th European Conference, Zurich, Switzerland, September 6–12, 2014, Proceedings, Part V 13. pp. 740–755. Springer (2014) **9**
32. Lin, Z., Liu, C., Zhang, R., Gao, P., Qiu, L., Xiao, H., Qiu, H., Lin, C., Shao, W., Chen, K., et al.: Sphinx: The joint mixing of weights, tasks, and visual embeddings for multi-modal large language models. arXiv preprint arXiv:2311.07575 (2023) **3, 8, 23**
33. Liu, H., Li, C., Li, Y., Lee, Y.J.: Improved baselines with visual instruction tuning. arXiv preprint arXiv:2310.03744 (2023) **2**
34. Liu, H., Li, C., Li, Y., Li, B., Zhang, Y., Shen, S., Lee, Y.J.: Llava-next: Improved reasoning, ocr, and world knowledge (January 2024), <https://llava-vl.github.io/blog/2024-01-30-llava-next/> **2, 11, 12, 13, 25**
35. Liu, H., Li, C., Wu, Q., Lee, Y.J.: Visual instruction tuning. Advances in neural information processing systems **36** (2024) **2, 7, 9, 13**
36. Liu, Y., Chen, H., Shen, C., He, T., Jin, L., Wang, L.: Abcnet: Real-time scene text spotting with adaptive bezier-curve network. In: proceedings of the IEEE/CVF conference on computer vision and pattern recognition. pp. 9809–9818 (2020) **9**
37. Liu, Z., Mao, H., Wu, C.Y., Feichtenhofer, C., Darrell, T., Xie, S.: A convnet for the 2020s. In: Proceedings of the IEEE/CVF conference on computer vision and pattern recognition. pp. 11976–11986 (2022) **23**
38. Loshchilov, I., Hutter, F.: Decoupled weight decay regularization. arXiv preprint arXiv:1711.05101 (2017) **10**
39. Lu, J., Batra, D., Parikh, D., Lee, S.: Vilbert: Pretraining task-agnostic visiolinguistic representations for vision-and-language tasks. Advances in neural information processing systems **32** (2019) **24**
40. Mani, A., Yoo, N., Hinthorn, W., Russakovsky, O.: Point and ask: Incorporating pointing into visual question answering. arXiv preprint arXiv:2011.13681 (2020) **6**
41. Mottaghi, R., Chen, X., Liu, X., Cho, N.G., Lee, S.W., Fidler, S., Urtasun, R., Yuille, A.: The role of context for object detection and semantic segmentation in the wild. In: Proceedings of the IEEE conference on computer vision and pattern recognition. pp. 891–898 (2014) **9**
42. Nayef, N., Patel, Y., Busta, M., Chowdhury, P.N., Karatzas, D., Khlif, W., Matas, J., Pal, U., Burie, J.C., Liu, C.I., et al.: Icdar2019 robust reading challenge on multi-lingual scene text detection and recognition—rrc-mlt-2019. In: 2019 International conference on document analysis and recognition (ICDAR). pp. 1582–1587. IEEE (2019) **9**
43. Nayef, N., Yin, F., Bizid, I., Choi, H., Feng, Y., Karatzas, D., Luo, Z., Pal, U., Rigaud, C., Chazalon, J., et al.: Icdar2017 robust reading challenge on multi-lingual scene text detection and script identification-rrc-mlt. In: 2017 14th IAPR international conference on document analysis and recognition (ICDAR). vol. 1, pp. 1454–1459. IEEE (2017) **9**
44. Oquab, M., Darcet, T., Moutakanni, T., Vo, H., Szafraniec, M., Khalidov, V., Fernandez, P., Haziza, D., Massa, F., El-Nouby, A., et al.: Dinov2: Learning robust visual features without supervision. arXiv preprint arXiv:2304.07193 (2023) **23**
45. Pan, T., Tang, L., Wang, X., Shan, S.: Tokenize anything via prompting (2023) **24**
46. Peng, Z., Wang, W., Dong, L., Hao, Y., Huang, S., Ma, S., Wei, F.: Kosmos-2: Grounding multimodal large language models to the world. arXiv preprint arXiv:2306.14824 (2023) **2, 5, 6, 9, 11, 12, 13**

47. Pfitzmann, B., Auer, C., Dolfi, M., Nassar, A.S., Staar, P.: Doclaynet: A large human-annotated dataset for document-layout segmentation. In: Proceedings of the 28th ACM SIGKDD Conference on Knowledge Discovery and Data Mining. pp. 3743–3751 (2022) [9](#)
48. Plummer, B.A., Wang, L., Cervantes, C.M., Caicedo, J.C., Hockenmaier, J., Lazebnik, S.: Flickr30k entities: Collecting region-to-phrase correspondences for richer image-to-sentence models. In: Proceedings of the IEEE international conference on computer vision. pp. 2641–2649 (2015) [6](#), [9](#), [25](#)
49. Radford, A., Wu, J., Child, R., Luan, D., Amodei, D., Sutskever, I., et al.: Language models are unsupervised multitask learners. OpenAI blog **1**(8), 9 (2019) [4](#)
50. Ramanathan, V., Kalia, A., Petrovic, V., Wen, Y., Zheng, B., Guo, B., Wang, R., Marquez, A., Kovvuri, R., Kadian, A., Mousavi, A., Song, Y., Dubey, A., Mahajan, D.: PACO: Parts and attributes of common objects. In: arXiv preprint arXiv:2301.01795 (2023) [11](#)
51. Rasheed, H., Maaz, M., Shaji, S., Shaker, A., Khan, S., Cholakkal, H., Anwer, R.M., Xing, E., Yang, M.H., Khan, F.S.: Glamm: Pixel grounding large multimodal model. arXiv preprint arXiv:2311.03356 (2023) [2](#), [5](#), [6](#), [9](#), [12](#)
52. Rawles, C., Li, A., Rodriguez, D., Riva, O., Lillicrap, T.: Android in the wild: A large-scale dataset for android device control. arXiv preprint arXiv:2307.10088 (2023) [9](#)
53. Rezatofghi, H., Tsoi, N., Gwak, J., Sadeghian, A., Reid, I., Savarese, S.: Generalized intersection over union: A metric and a loss for bounding box regression. In: Proceedings of the IEEE/CVF conference on computer vision and pattern recognition. pp. 658–666 (2019) [11](#)
54. Shao, S., Li, Z., Zhang, T., Peng, C., Yu, G., Zhang, X., Li, J., Sun, J.: Objects365: A large-scale, high-quality dataset for object detection. In: Proceedings of the IEEE/CVF international conference on computer vision. pp. 8430–8439 (2019) [9](#)
55. Shtedritski, A., Rupprecht, C., Vedaldi, A.: What does clip know about a red circle? visual prompt engineering for vlms. arXiv preprint arXiv:2304.06712 (2023) [5](#)
56. Su, W., Zhu, X., Cao, Y., Li, B., Lu, L., Wei, F., Dai, J.: Vi-bert: Pre-training of generic visual-linguistic representations. arXiv preprint arXiv:1908.08530 (2019) [24](#)
57. Tancik, M., Srinivasan, P., Mildenhall, B., Fridovich-Keil, S., Raghavan, N., Singhal, U., Ramamoorthi, R., Barron, J., Ng, R.: Fourier features let networks learn high frequency functions in low dimensional domains. *Advances in Neural Information Processing Systems* **33**, 7537–7547 (2020) [8](#), [23](#)
58. Touvron, H., Martin, L., Stone, K., Albert, P., Almahairi, A., Babaei, Y., Bashlykov, N., Batra, S., Bhargava, P., Bhosale, S., et al.: Llama 2: Open foundation and fine-tuned chat models. arXiv preprint arXiv:2307.09288 (2023) [4](#), [9](#)
59. Veit, A., Matera, T., Neumann, L., Matas, J., Belongie, S.: Coco-text: Dataset and benchmark for text detection and recognition in natural images. arXiv preprint arXiv:1601.07140 (2016) [11](#)
60. Wang, J., Zhang, P., Chu, T., Cao, Y., Zhou, Y., Wu, T., Wang, B., He, C., Lin, D.: V3det: Vast vocabulary visual detection dataset. arXiv preprint arXiv:2304.03752 (2023) [9](#)
61. Wang, W., Shi, M., Li, Q., Wang, W., Huang, Z., Xing, L., Chen, Z., Li, H., Zhu, X., Cao, Z., et al.: The all-seeing project: Towards panoptic visual recognition and understanding of the open world. arXiv preprint arXiv:2308.01907 (2023) [24](#)
62. Wang, W., Chen, Z., Chen, X., Wu, J., Zhu, X., Zeng, G., Luo, P., Lu, T., Zhou, J., Qiao, Y., et al.: Visionllm: Large language model is also an open-ended decoder

- for vision-centric tasks. *Advances in Neural Information Processing Systems* **36** (2024) [4](#)
63. Wang, X., Li, S., Kallidromitis, K., Kato, Y., Kozuka, K., Darrell, T.: Hierarchical open-vocabulary universal image segmentation. *Advances in Neural Information Processing Systems* **36** (2024) [5](#)
64. Wu, J., Wang, J., Yang, Z., Gan, Z., Liu, Z., Yuan, J., Wang, L.: Grit: A generative region-to-text transformer for object understanding. *arXiv preprint arXiv:2212.00280* (2022) [24](#)
65. Yang, J., Zhang, H., Li, F., Zou, X., Li, C., Gao, J.: Set-of-mark prompting unleashes extraordinary visual grounding in gpt-4v. *arXiv preprint arXiv:2310.11441* (2023) [7](#)
66. Yao, Y., Zhang, A., Zhang, Z., Liu, Z., Chua, T.S., Sun, M.: Cpt: Colorful prompt tuning for pre-trained vision-language models. *arXiv preprint arXiv:2109.11797* (2021) [5](#)
67. You, H., Zhang, H., Gan, Z., Du, X., Zhang, B., Wang, Z., Cao, L., Chang, S.F., Yang, Y.: Ferret: Refer and ground anything anywhere at any granularity. *arXiv preprint arXiv:2310.07704* (2023) [2](#), [3](#), [5](#), [11](#), [12](#), [13](#)
68. Yu, F., Tang, J., Yin, W., Sun, Y., Tian, H., Wu, H., Wang, H.: Ernie-vil: Knowledge enhanced vision-language representations through scene graphs. In: *Proceedings of the AAAI Conference on Artificial Intelligence*. vol. 35, pp. 3208–3216 (2021) [24](#)
69. Yu, L., Poirson, P., Yang, S., Berg, A.C., Berg, T.L.: Modeling context in referring expressions. In: *Computer Vision—ECCV 2016: 14th European Conference, Amsterdam, The Netherlands, October 11–14, 2016, Proceedings, Part II 14*. pp. 69–85. Springer (2016) [6](#), [9](#), [13](#)
70. Yuan, Y., Li, W., Liu, J., Tang, D., Luo, X., Qin, C., Zhang, L., Zhu, J.: Osprey: Pixel understanding with visual instruction tuning. *arXiv preprint arXiv:2312.10032* (2023) [2](#), [3](#), [5](#), [9](#), [10](#), [11](#), [12](#), [13](#)
71. Yuliang, L., Lianwen, J., Shuaitao, Z., Sheng, Z.: Detecting curve text in the wild: New dataset and new solution. *arXiv preprint arXiv:1712.02170* (2017) [9](#)
72. Zellers, R., Bisk, Y., Farhadi, A., Choi, Y.: From recognition to cognition: Visual commonsense reasoning. In: *The IEEE Conference on Computer Vision and Pattern Recognition (CVPR)* (June 2019) [6](#), [10](#), [24](#)
73. Zhang, S., Sun, P., Chen, S., Xiao, M., Shao, W., Zhang, W., Chen, K., Luo, P.: Gpt4roi: Instruction tuning large language model on region-of-interest. *arXiv preprint arXiv:2307.03601* (2023) [2](#), [5](#), [11](#), [12](#), [24](#), [25](#)
74. Zhao, L., Yu, E., Ge, Z., Yang, J., Wei, H., Zhou, H., Sun, J., Peng, Y., Dong, R., Han, C., et al.: Chatspot: Bootstrapping multimodal llms via precise referring instruction tuning. *arXiv preprint arXiv:2307.09474* (2023) [2](#), [3](#), [5](#), [11](#)
75. Zhong, X., Tang, J., Yepes, A.J.: Publaynet: largest dataset ever for document layout analysis. In: *2019 International Conference on Document Analysis and Recognition (ICDAR)*. pp. 1015–1022. IEEE (2019) [9](#)
76. Zhou, B., Zhao, H., Puig, X., Xiao, T., Fidler, S., Barriuso, A., Torralba, A.: Semantic understanding of scenes through the ade20k dataset. *International Journal of Computer Vision* **127**, 302–321 (2019) [9](#)
77. Zhou, Q., Yu, C., Zhang, S., Wu, S., Wang, Z., Wang, F.: Regionblip: A unified multi-modal pre-training framework for holistic and regional comprehension. *arXiv preprint arXiv:2308.02299* (2023) [2](#)
78. Zhu, D., Chen, J., Shen, X., Li, X., Elhoseiny, M.: Minigpt-4: Enhancing vision-language understanding with advanced large language models. *arXiv preprint arXiv:2304.10592* (2023) [2](#)

79. Zhu, Y., Groth, O., Bernstein, M., Fei-Fei, L.: Visual7w: Grounded question answering in images. In: Proceedings of the IEEE conference on computer vision and pattern recognition. pp. 4995–5004 (2016) [6](#), [9](#), [10](#)
80. Zou, X., Yang, J., Zhang, H., Li, F., Li, L., Wang, J., Wang, L., Gao, J., Lee, Y.J.: Segment everything everywhere all at once. Advances in Neural Information Processing Systems **36** (2024) [5](#)

Appendix

A More Details of Architecture

Image Encoder. In general, the image encoder can be any network that outputs a $C \times H \times W$ image embedding. Motivated by scalability and access to strong pre-training, we employ a Mixture of Visual Experts (MoV) with mixed scales and high-resolution sub-images to process high-resolution inputs [18, 32]. Specifically, we use two complementary vision encoders: DINOv2 [44] and CLIP-ConvNeXt [37], to capture a diverse visual representation. During training, all images are by default scaled and zero-padded to a high resolution of 448×448 , and then divided into four 224×224 sub-images. For images with large aspect ratios, such as 2 : 1, this results in fully-padded sub-images that are filled entirely with zero-value pixels. To address this issue, we follow a strategy [18] that involves using a learnable skip token to replace the fully-padded sub-image. This provides explicit relative positional information, enabling Language Learning Models (LLMs) to identify the positions between useful sub-images more effectively.

Visual Prompt Encoder. In Fig. 7, we present our approach for the integration of multiple visual prompts (VPs) into the visual prompt encoder. Specifically, for point-type inputs, we represent VPs as the sum of a positional encoding [57] of the point’s coordinates. For box-type inputs, inspired by [24], VPs are conceptualized as the aggregate of positional encodings for the coordinates of both the ‘top-left corner’ and the ‘bottom-right corner’. We then proceed to dynamically assess the efficacy of the feature set associated with each VP, applying one of two learned embeddings to indicate the VP’s validity. To further delineate and model the positions of the center point, the ‘top-left corner’, and the ‘bottom-right corner’, we allocate three distinct learned embeddings for each. The culmination of this process involves the incorporation of an MLP as the output layer, tasked with generating the final embeddings of the visual prompts with a dimensionality of 512.

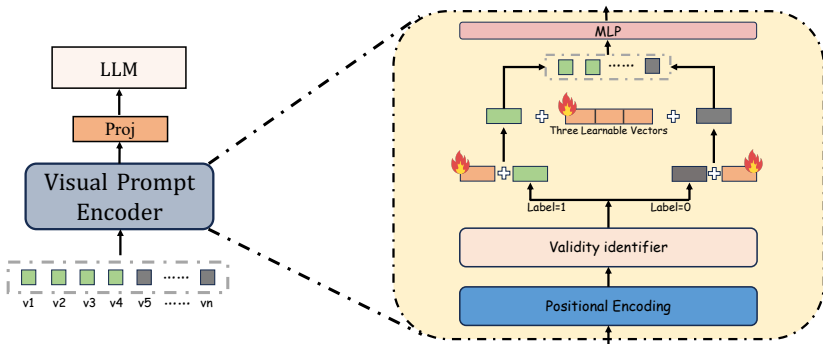


Fig. 7: Details of the visual prompt encoder.

Table 10: Comparison of various methods on the Visual Genome dataset.

Method	Prompt Type	Visual Genome	
		METEOR	CIDEr
GRiT [64]	Bounding Box	17.1	142.0
GPT4ROI-7B [73]	Bounding Box	17.4	145.2
GPT4ROI-13B [73]	Bounding Box	17.6	146.8
ASM [61]	Bounding Box	18.0	145.1
SCA(GPT2-774M) [20]	(8 Caption + 6 Task) Tokens	17.4	148.8
SCA(LLama-3B) [20]	(8 Caption + 6 Task) Tokens	17.4	149.8
TAP(ViT-B) [45]	1 Semantic Token	17.4	149.2
TAP(ViT-L) [45]	1 Semantic Token	17.5	150.7
SPHINX-V(ours)	Bounding Box	24.3	197.3

Table 11: Validation Accuracy on VCR dataset.

Model	Q → A (%)	QA → R (%)	Q → AR (%)
ViLBERT [39]	72.4	74.5	54.0
Unicoder-VL [28]	72.6	74.5	54.5
VLBERT-L [56]	75.5	77.9	58.9
ERNIE-ViL-L [68]	78.52	83.37	65.81
VILLA-L [17]	78.45	82.57	65.18
GPT4RoI-7B [73]	87.4	89.6	78.6
ViP-LLaVA-Base-7B [3]	87.66	89.80	78.93
SPHINX-V(Ours)	89.65	90.23	89.63

B More Experiments

B.1 Brief Region Description

To further evaluate the captioning capability of SPHINX-V, we conducted tests on the evaluation set of Visual Genome [25]. As the comparison results shown in Tab. 10, our SPHINX-V model exhibits promising performance compared to other models that utilize various types of prompts. It achieves a METEOR score of 24.3 and a CIDEr score of 197.3, significantly outperforming the state-of-the-art TAP(ViT-L) [45] approach by 6.8 and 46.6, respectively. These results highlight the superior capability of our model in generating semantically relevant descriptions for object regions.

B.2 Region-Level Reasoning

To evaluate the reasoning capabilities of SPHINX-V, we utilized the Visual Commonsense Reasoning (VCR) dataset [72], a challenging benchmark designed to assess a model’s high-level cognitive and commonsense reasoning abilities within context. The VCR dataset comprises multiple-choice questions that require an understanding of the scene depicted in an image. Each question (Q) is accompanied by four possible answers (A), necessitating the model to not only identify

the correct answer but also provide a rationale (R) supporting its selection. This process underscores the model’s proficiency in interpreting and justifying visual elements within specific contexts, with accuracy serving as the evaluation metric. Following the evaluation approach employed in LLaVA-ViP [34] and GPT4RoI [73], we fine-tuned our SPHINX-V model using the training set of VCR. As shown in the comparison results in Tab. 11, our model achieves the highest performance scores of 89.65%, 90.23%, and 89.63% across three distinct evaluation methods, respectively, showcasing its proficiency in visual common-sense reasoning.

C More Details of Dataset

In this section, we outline our methodology for reconstructing public grounding datasets and our application of GPT-4V to produce instruction-based data spanning a variety of domains, leading to the development of the MDVP Dataset. Fig. 8 depicts an example from our Inverse-Grounding dataset. Sec. C.2 showcase the prompts used to generate data across these diverse domains with GPT-4V.

C.1 Examples of Inverse Grounding

Using two sample images from the Flickr30k dataset [48] as illustrations, the phrase grounding task is defined as identifying the bounding boxes in an image that correspond to various referring phrases, based on a given ground truth (gt) sentence. In a twist on this task, we invert the annotation process: the model, provided with bounding boxes, is tasked with generating the corresponding gt sentence. This process is depicted in Fig. 8.

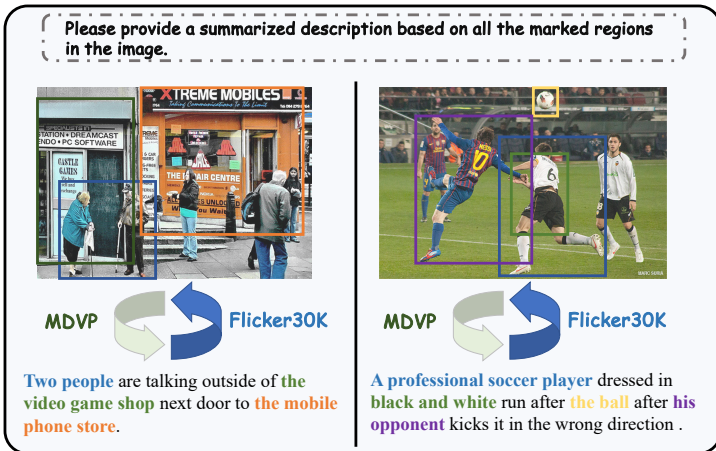


Fig. 8: Examples of Inverse-Grounding data.

C.2 Prompts for Data Generation

We carefully designed prompts to facilitate data generation by GPT-4V, assigning it various roles and embedding category-specific information within these prompts. Table 12 outlines a universal prompt template applied across different domains. Meanwhile, Tables 13, 14, 15, 16, and 17 detail prompts tailored to specific domains. An illustrative example of GPT-4V’s response during data generation is provided in Table 18.

```
image =
```



```
messages = {"role": "system", "content": In the image, I have marked
each visual object with a green point, and each is identified by a white
numeric ID against a black background.

The categories of visual objects are as follows:
<Mark 1>: dog
<Mark 2>: bed
<Mark 3>: mattress
<Mark 4>: pillow

Your analysis will revolve around four main functions:
<Role>

I will now supply you with specific output templates for content corresponding
to the four roles. Please adhere strictly to these templates when generating
content, refraining from making any additional alterations, including the
insertion of extra spaces or line breaks. Adhering to this guideline is extremely
crucial.
Format:
<Format>

Proceed with your analysis, keeping the language natural and clear.}
```

Table 12: The public prompt template used to feed to GPT-4V for data generation. Public prompts for different domains exhibit slight variations. For instance, in the screen-shot domain, "In the image" is modified to "In the screen-shot". The highlighted **<Role>** and **<Format>** in red are domain-specific.

Role

<Role 1 (Short Description)> Provide a succinct and clear description for each marked region, ensuring each description stands independently without reference or comparison to others.

<Role 2 (Detailed Description)> For each marked region in the image, please provide as detailed a description as possible using natural language. Highlight the object's category, type, color, and additional attributes such as location, condition, and any relevant details. Envision yourself observing each region directly and convey your observations as thoroughly and promptly as possible. A minimum of 30 words is required in your description. Treat each mark as a unique and separate entity, requiring a full description exclusive to that mark only.

<Role 3 (Inter-Relationship Analysis)> Delve into and analyze the relationships between the marked regions. In your analysis, reference specific areas using identifiers like **<Mark 1>**, **<Mark 2>**, etc. Elucidate the links and common features among these areas, which might encompass aspects such as their spatial arrangement, inherent qualities, underlying principles, resemblances, variances, contextual ties, or notable discrepancies. Should you find certain relational aspects insignificant or lacking in noteworthy content, omit them from your discussion. In instances where a marked region stands apart without clear ties to others, highlight its distinctiveness and provide a detailed description of this unique object or area.

<Role 4 (Q&A and Conversations)> Dive deeper into the detailed content and intricacies of every marked regions, and interconnections among multiple marked regions. Employ identifiers such as **<Mark 1>**, **<Mark 2>**, etc., to specify each area in your inquiries and responses. Assist in formulating question-answer pairs that focus on either a single target area or multiple target areas, aiming to develop a rich dialogue dataset (comprising at least 4 Q&A pairs). Ensure that the questions you craft inquire about one or more specified **<Mark>**s.

Format

Role 1

<Mark 1>: Your Short Description

...

<Mark N>: Your Short Description

Role 2

<Mark 1>: Your Comprehensive Description

...

<Mark N>: Your Comprehensive Description

Role 3

<Mark 1><Mark 2>...<Mark N>: Your Detailed Analysis

...

<Mark 1><Mark 2>...<Mark N>: Your Detailed Analysis

Role 4

{"question": [Your created Question], "Answer": [Your created answer]}

...

{"question": [Your created Question], "Answer": [Your created answer]}

Table 13: The **<Role>** and **<Format>** prompt template used for natural images domain.

Role

<Role 1 (Detailed Analysis and Description)> First, you need to deeply understand the page content presented by the entire screenshot, and then thoroughly examine and explain the content and purpose of the highlighted area. Provide a comprehensive description of its features, layout and functionality. Specify if the area is interactive (such as a clickable button or search bar), and describe the result or action that occurs upon interaction. If the highlighted area contains text, analyze whether it is a hyperlink, and the meaning of the text and its intended function. To ensure precise and detailed descriptions for the marked regions, please observe the following guidelines. Avoid mentioning the green rectangle or numeric ID of the marks I placed on the image, as they are not significant. Treat each mark as a unique and separate entity, requiring a full description exclusive to that mark only. A minimum of 30 words is required in your description.

<Role 2 (Q&A and Conversations)> Dive deeper into the detailed content and intricacies of every marked regions, and interconnections among multiple marked regions. Employ identifiers such as **<Region 1>**, **<Region 2>**, etc., to specify each area in your inquiries and responses. Assist in formulating question-answer pairs that focus on either a single target area or multiple target areas, aiming to develop a rich dialogue dataset (comprising at least 4 Q&A pairs). Ensure that the questions you craft inquire about one or more specified **<Region>**s.

Table 14: The **<Role>** prompt template used for screenshots domain. The **<Format>** can be referenced from natural images domain in Tab.13.

Role

<Role 1 (Detailed Region Description)> For each marked region in the image, provide a thorough description using natural language. First, referring to the categories of visual objects I provided you with, you need to tell me what the marked region is. Then, do your best to describe the content, characteristics, and function of the marked area. If the marked area is a text paragraph, you should first understand the content of the text, and then summarize the main idea. If the marked area is an image, you need to describe the content of the image in detail, as well as why this image is included in the document.

To ensure precise and detailed descriptions for the marked regions, please observe the following guidelines. Avoid mentioning the green rectangle or numeric ID of the marks I placed on the image, as they are not significant. Treat each mark as a unique and separate entity, requiring a full description exclusive to that mark only.

<Role 2 (Q&A and Conversations)> Dive deeper into the detailed content and intricacies of every marked regions, and interconnections among multiple marked regions. Employ identifiers such as **<Region 1>**, **<Region 2>**, etc., to specify each area in your inquiries and responses. Assist in formulating question-answer pairs that focus on either a single target area or multiple target areas, aiming to develop a rich dialogue dataset (comprising at least 4 Q&A pairs). Ensure that the questions you craft inquire about one or more specified **<Region>**s.

Table 15: The **<Role>** prompt template used for document domain. The **<Format>** can be referenced from natural images domain in Tab.13.

Role

<Role 1 (Detailed Region Description)> For each marked region in the image, I'd like you to give a detailed description, as if you were examining it in person. First refer to the OCR results of the specified area I provided to clarify the text content. Then, delve into the characteristics of the text, including the font style and its exact location within the image. I'd also appreciate insights into the background context of the region and an analysis of why the text is present—its intended purpose. Please ensure your explanation is clear and straightforward.

To ensure precise and detailed descriptions for the marked regions, please observe the following guidelines. Avoid mentioning the red polygon or numeric ID of the marks I placed on the image, as they are not significant. Treat each mark as a unique and separate entity, requiring a full description exclusive to that mark only.

<Role 2 (Q&A and Conversations)> Dive deeper into the detailed content and intricacies of every marked regions, and interconnections among multiple marked regions. Employ identifiers such as **<Region 1>**, **<Region 2>**, etc., to specify each area in your inquiries and responses. Assist in formulating question-answer pairs that focus on either a single target area or multiple target areas, aiming to develop a rich dialogue dataset (comprising at least 4 Q&A pairs). Ensure that the questions you craft inquire about one or more specified **<Region>**s.

Table 16: The **<Role>** prompt template used for OCR-spotting domain. The **<Format>** can be referenced from natural images domain in Tab.13.

Role

<Role 1 (Detailed Region Description)> For each marked region in the image, please provide as detailed a description as possible using natural language. Carefully observe and analyze the content and details of each panel I have marked. Tell me as best you can what the content and purpose of each marked area is, including the content of figure and the text. Envision yourself observing each region directly and convey your observations as thoroughly and promptly as possible. Treat each mark as a unique and separate entity, requiring a full description exclusive to that mark only. A minimum of 30 words is required in your description.

<Role 2 (Inter-Relationship Analysis)> Delve into and analyze the relationships between the marked regions. In your analysis, reference specific areas using identifiers like **<Region 1>**, **<Region 2>**, etc. Elucidate the links and common features among these areas, which might encompass aspects such as their spatial arrangement, reading order and contextual ties.

<Role 2 (Q&A and Conversations)> Dive deeper into the detailed content and intricacies of every marked regions, and interconnections among multiple marked regions. Employ identifiers such as **<Region 1>**, **<Region 2>**, etc., to specify each area in your inquiries and responses. Assist in formulating question-answer pairs that focus on either a single target area or multiple target areas, aiming to develop a rich dialogue dataset (comprising at least 4 Q&A pairs). Ensure that the questions you craft inquire about one or more specified **<Region>**s.

Table 17: The **<Role>** prompt template used for multi-panels images domain. The **<Format>** can be referenced from natural images domain in Tab.13.

Response

<Role 1 (Short Description)>

<Mark 1>: Light brown dog sleeping peacefully on a bed.

<Mark 2>: A neatly arranged bed with light blue floral patterns.

<Mark 3>: Cream-colored mattress exposed at the edge of the bed.

<Mark 4>: Soft grey pillow partially tucked under a sleeping dog's head.

<Role 2 (Detailed Description)>

<Mark 1>: The image displays a light brown adult dog with a closed eyes and relaxed ears, lying on its side, comfortably asleep. The dog appears to be in a serene state of rest, with its head gently resting on a pillow, hinting at the trust and safety it feels in its environment.

<Mark 2>: This mark points to a well-kept bed covered with light blue sheets that exhibit a delicate floral design. The sheets seem smooth and unwrinkled, suggesting the bed was recently made or is well-maintained, providing a cozy resting place.

<Mark 3>: An exposed corner of a cream-colored mattress is visible here, revealing its thick, sturdy build. The mattress looks to be in good condition, with a soft upper layer that likely contributes to a comfortable sleeping experience.

<Mark 4>: Here, we see a soft grey pillow with a smooth texture. It appears to be of a thickness that provides ample support for comfort. The pillow is partially tucked under the sleeping dog's head, indicating its use for rest.

<Role 3 (Inter-Relationship Analysis) >

<Mark 1><Mark 2>: These marks indicate a relationship of proximity and usage. The dog <Mark 1> is resting on the bed <Mark 2>, which implies the bed's purpose in the household as a place for relaxation and sleep.

<Mark 1><Mark 4>: There is a direct interaction here; the dog <Mark 1> has its head on the pillow <Mark 4>, showcasing the pillow's function as a support for comfort and the dog's apparent enjoyment of this provision.

<Mark 2><Mark 3>: The bed <Mark 2> is made up with sheets that likely cover the mattress <Mark 3>, indicating that the mattress is part of the bed setup, essential for providing a comfortable sleeping surface.

<Mark 3><Mark 4>: There is no direct relationship between the mattress <Mark 3> and the pillow <Mark 4> other than they both contribute to the overall comfort of the sleeping area. Each serves a different aspect of comfort and support.

<Role 4 (Q&A and Conversations)>

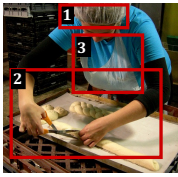
```
{ "question": "What color is the dog at <Mark 1>?", "answer": "The dog at <Mark 1> is light brown." }
```

```
{ "question": "Describe the design of the bed's sheets at <Mark 2>.", "answer": "The sheets at <Mark 2> have a light blue color with a floral design." }
```

```
{ "question": "What can be said about the condition of the mattress at <Mark 3>?", "answer": "The mattress at <Mark 3> appears to be in good condition and sturdy." }
```

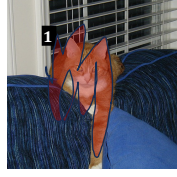
```
{ "question": "How does the pillow at <Mark 4> contribute to the dog's comfort?", "answer": "The pillow at <Mark 4> provides support and comfort for the dog's head while it sleeps." }
```

Table 18: An example response from GPT-4V during data generation.



Please analyze the relationship between all marked points in the image.

The three marked regions are all components of a bakery or kitchen setting, with <Region 1> and <Region 3> being attire worn by the individual at <Region 2>, which is engaged in food preparation.



Please provide a brief description of each marked region in the image.

Orange and white cat sitting on furniture.



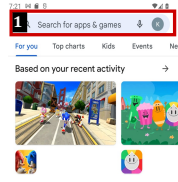
Please provide a detailed description of <Region 1> in the image.

A person is shown with a bandage wrapped around the arm, indicating a recent injury or ailment.



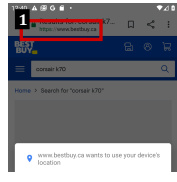
Please analyze the relationship between all marked regions in the image.

The marked regions collectively illustrate themes related to social and emotional learning, with a focus on managing "ADHD" in children.



Please provide a detailed description of <Region 1> in the image.

This area appears to be a search bar at the top of a settings menu, typically used for finding specific settings quickly.



Please provide a detailed description of <Region 1> in the image.

<Region 1>: The text "\https://www.bestbuy.ca" is a URL, suggesting that it is a hyperlink to the Best Buy Canada website. It is typically interactive and would direct a user to that webpage when clicked.



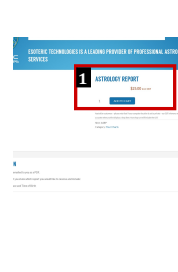
What phrase do <Mark 1> and <Mark 2> together form and what language is it?

Together, <Mark 1> and <Mark 2> form the phrase 'SELAMAT Datang' in Malay, which means 'Welcome' in English.



What does the complete text on the signboard suggest about the location?

The complete text 'SEACREST BEACH' suggests that the signboard is identifying a beach named Seacrest, which is likely a destination or point of interest for visitors.



Please provide a detailed description of <Region 1> in the image.

This area likely represents a shopping cart icon, which is commonly used on e-commerce websites to indicate where users can view items they have selected for purchase. It is typically interactive, and clicking on it would take the user to a page where they can review their chosen products, adjust quantities, remove items, or proceed to checkout.



Please provide a detailed description of <Region 1> in the image.

This region appears to be a part of a digital map interface, specifically highlighting a section of text that provides directions. The text is likely part of a list of directions or a route that can be followed, and it is presented in a way that indicates it is interactive, possibly clickable, allowing the user to navigate to the specified location when selected.



Please provide a detailed description of each marked region in the image.

"<Region 1>: This region appears to be a section-header that reads '\CONSOLIDATED BALANCE SHEETS AT DECEMBER 31'. This header indicates that the section below will present the consolidated balance sheets of an entity for the year ending on December 31 of the current year.



"What are the stable phases depicted in <Region 1>?"

The stable phases depicted in <Mark 1> are the molecular-BEC phase (P(S)) and the normal phase (N(S)) of a pairing gas with a wide Fock's resonance.

Fig. 9: Additional visual examples of SPHINX-V utilizing arbitrary-shaped visual prompts across multiple domains.